RSC Advances

PAPER

View Article Online
View Journal | View Issue



Cite this: *RSC Adv.*, 2022, **12**, 35032

# Radiolabeled albumin through $S_NAr$ of cysteines as a potential pretargeting theranostic agent†

Niklas H. Fischer,[ab] Sara I. Lopes van den Broek,[c] Matthias M. Herth[*cd] and Frederik Diness[*ab]

Received 11th October 2022
Accepted 23rd November 2022

DOI: 10.1039/d2ra06406e

rsc.li/rsc-advances

Human serum albumin (HSA) has been shown to be a promising tumor targeting vector and target for generating theranostics by bioconjugation. Unstable chemical conjugation to HSA *via* a cysteine (Cys34) by reversible Michael additions is most commonly applied for this purpose. Herein, we describe utilization of our recently developed site-selective irreversible $S_NAr$ conjugation to Cys34 using perfluorobenzene sulfonyl derivatives to introduce a *trans*-cyclooctene (TCO) handle. The TCO could then be bioorthogonally ligated within minutes through an inverse-electron demand Diels–Alder reaction (IEDDA) to tetrazines (Tzs) containing a radionuclide. The methodology opens up a wide range of chemistries including pretargeting, 'click-to-release' tumor selective drug delivery or ultra-fast and complete conjugation of any drug. The proof-of-principle study demonstrated that the conjugation chemistry is feasible, robust and easy to carry out, being promising for pretargeted imaging and therapy studies as well as selective drug delivery using HSA.



## Introduction

Human serum albumin (HSA) is the most abundant protein in the blood serum. It has emerged as a versatile targeting vector for theranostic (diagnostic and therapeutic) strategies. HSA has for example been used to diagnose and treat rheumatoid arthritis, cancer, diabetes, and infectious diseases. With respect to imaging, HSA found widespread application in blood imaging and angiography.[1] For example, $^{131}$I-labeled human serum albumin is a Food and Drug Administration approved drug to measure the blood volume.[2] Recently, HSA has also been used to locate sentinel lymph nodes (LNs) in various animal models including a metastatic breast cancer model.[3,4] The ability to accurately locate sentinel LNs using non-invasive imaging technologies such as single-photon emission computed tomography (SPECT) or positron emission tomography (PET) would greatly assist tumor staging.[5,6] From a general point of view, HSA accumulates in leaky cancerous tissues due to the enhanced permeability and retention (EPR) effect (Fig. 1A).[7] Even though controversial, the EPR effect has recently been shown to be present in some cancer patients – in an interpatient and intratumor dependent manner; tumor uptake varied from 5% to 50% ID per kg within the same tumor type.[8–11] Interestingly, HSA is able to image LNs and EPR positive tumors using an *in vivo* labeling strategy (Fig. 1A).[1,12] In this approach, endogenous albumin is targeted *in vivo* with Evans blue (EB). This is possible as EB possesses a high affinity towards HSA.[13] However, the selectivity over other proteins is low. For example, EB also binds plasma proteins in the post-albumin fraction and not all EB injected binds to proteins, *i.e.*, there is also unbound EB present in blood.[14]

The inverse-electron demand Diels–Alder reaction (IEDDA) of a tetrazine (Tz) with a *trans*-cyclooctene (TCO) is a bioorthogonal "click" reaction which has attracted great interest for pretargeted strategies.[11,15,16] This ligation is ultrafast, used agents can easily be modified, and the ligation has already successfully been applied *in vivo* for imaging and targeted radionuclide therapies. For example, Tzs with radionuclide theranostic pairs, *e.g.* carbon-11, fluorine-18, gallium-68, scandium-44, technetium-99m, actinium-225, lead-212, iodine-125, and lutetium-177, exist.[17–26] Furthermore, the ligation has also attracted interest for conventional labeling approaches as it allows to tag a peptide or protein within seconds, at room temperature – even at tracer doses (μM precursor concentrations).[27] These conditions allow to label the target vector without additional purification. Finally, the Tz ligation has been used for 'click-to-release' drug delivery approaches – even in the clinic.[28–30] In an animal model, 'click-

[a]*Department of Chemistry, Faculty of Science, University of Copenhagen, Universitetsparken 5, Copenhagen 2100, Denmark. E-mail: diness@ruc.dk*

[b]*Department of Science and Environment, Roskilde University, Universitetsparken 1, Roskilde 4000, Denmark*

[c]*Department of Drug Design and Pharmacology, Faculty of Health and Medical Sciences, University of Copenhagen, Jagtvej 160, Copenhagen 2100, Denmark. E-mail: matthias.herth@sund.ku.dk*

[d]*Department of Clinical Physiology, Nuclear Medicine & PET, Rigshospitalet, Blegdamsvej 9, Copenhagen 2100, Denmark*

† Electronic supplementary information (ESI) available. See DOI: https://doi.org/10.1039/d2ra06406e

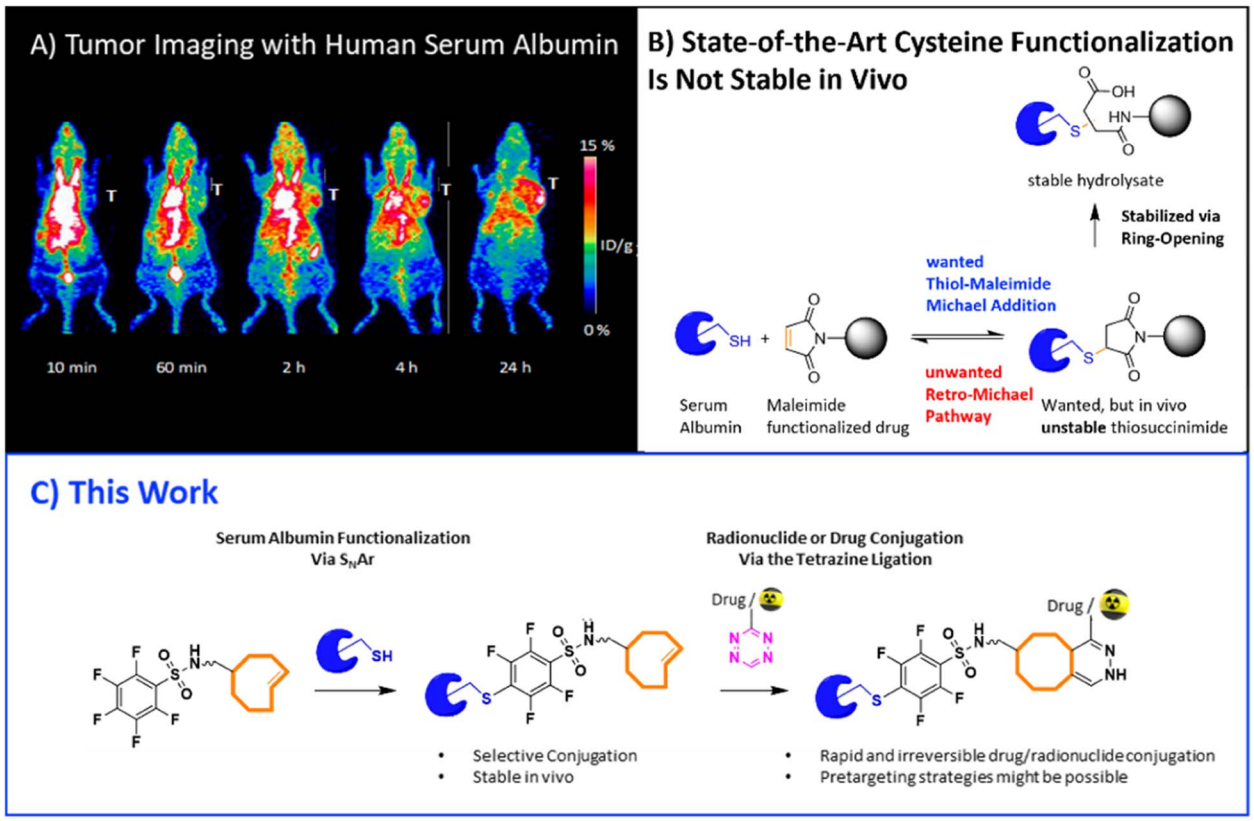


Fig. 1 (A) PET images of $^{64}$Cu-labeled human serum albumin (HSA) show the ability to accumulate in tumorous leaky tissue. (Figure adapted from Niu *et al.*[1]). (B) Challenges of current thiol-maleimide Michael additions used to functionalize cysteines. (C) Objective of this study: stable functionalization of HSA *via* conjugation of a perfluoro-benzene sulfonyl derivative to Cys34 is displayed. A subsequent Tz ligation allows for a wide range of chemistries including pretargeting and ultra-fast and complete conjugation of any drug. The illustration shows the synthesis of an HSA-TCO construct based on the $S_NAr$ reaction and subsequent Tz ligation with a radiolabeled tetrazine probe.

to-release' increased median survival from 26 days to 50 days compared to conventional therapy.[31]

Introducing a *trans*-cyclooctene (TCO) handle to a protein of interest requires mild orthogonal chemistries avoiding acidic conditions. Herein, we describe a novel strategy to label HSA easily and selectively for conventional and pretargeted purposes. For this purpose, we aimed to use the free and highly nucleophilic cysteine handle (Cys34) available in HSA. Most commonly, conjugation to this Cys residue is conducted *via* a Michael addition to an electrophilic maleimide.[32] However, these reactions are reversible, frequently providing low yields, and the succinimide product requires a subsequent hydrolysis step to attain stability (Fig. 1B). We have recently shown that nucleophilic aromatic substitutions ($S_NAr$) between Cys residues and electrophilic perfluorobenzene sulfonyl derivatives are quick, robust, compatible with biological conditions, and irreversible (Fig. 1C).[33] Furthermore, these fluoroaryls react site-selectively with the free thiol of Cys34. In order to provide a bioorthogonal handle to HSA, we envisioned to link a *trans*-cyclooctene (TCO) moiety to this perfluorobenzene sulfonyl derivative. This TCO would allow a subsequent Tz ligation and as such, the possibility to introduce any radionuclide, drug or imaging probe within seconds, allow possibly for pretargeting with higher selectivity than EB approaches and in a slightly modified version for drug delivery 'click-to-release' approaches.

## Results and discussion

In order to conjugate TCOs to HSA, we decided to synthesize two pentafluorobenzene TCO-bearing moieties. Linker length was varied in order to investigate if the linker length or polarity influences the ability of Tzs to interact with the HSA conjugated TCOs. The lipophilic linker was based on a simple, linear trimethylene structure whereas the more polar linker was additionally based on three PEG units and a triazole moiety. Compound **1** was synthesized from commercially available amine-functionalized TCO and pentafluorobenzenesulfonyl chloride. In contrast, compound **2** was prepared from *N*-(2-(2-(2-(2-azidoethoxy)ethoxy)ethoxy)ethyl)-2,3,4,5,6-pentafluorobenzenesulfonamide (**2a**), which was synthesized according to Psimadas *et al.*[34] and propiolic acid in a yield of approx. 25% *via* a copper(I)-catalyzed azide–alkyne cycloaddition, CuAAC (not shown).[35–37] Compounds **1** and **2** were then conjugated with HSA without further purification. The $S_NAr$ proceeded in 3 : 7 mixture of acetonitrile and PBS buffer, pH 8.5, to yield **HSA1** and **HSA2**. Fig. 2A and B display the applied strategy. LC-MS analysis revealed full conversion of HSA after

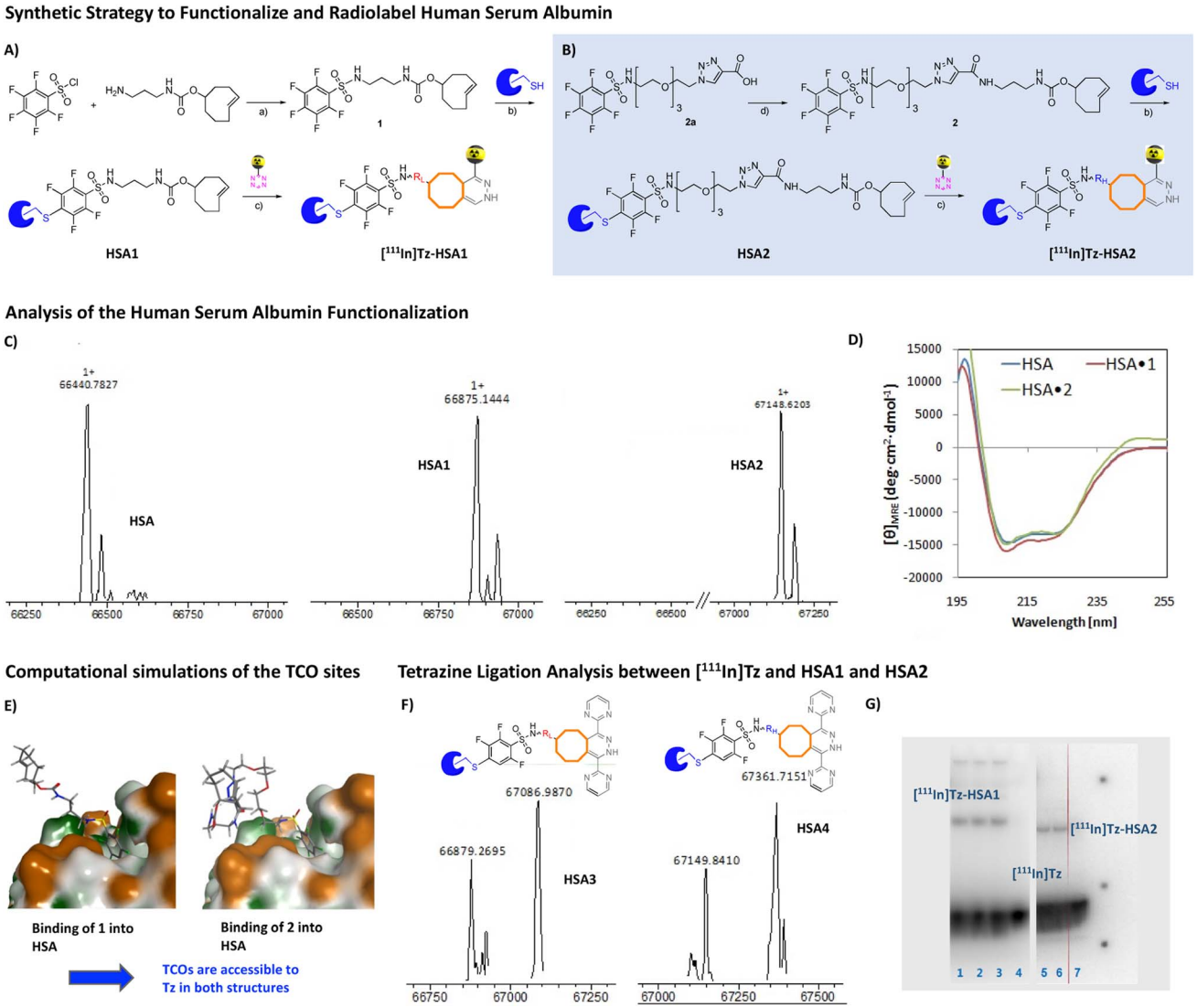


Fig. 2 (A + B) Synthetic scheme to functionalize and label human serum albumin (HSA); (a) $CH_2Cl_2$, 2,6-lutidine, room temperature, 0.5 h, (b) MeCN/PBS (3 : 7), 31 °C for 24 h, (c) MeCN, room temperature for 15 min, (d) TCO-amine, PyBOP, DIPEA, $CH_2Cl_2$, room temperature for 50 min; (C) deconvoluted MS spectrum of HSA, **HSA1** and **HSA2** displays full conversion of HSA during the $S_NAr$; (D) the circular dichroism (CD) spectra of HSA, **HSA1**, and **HSA2** confirms that the α-helical structure of HSA was retained after modification with **1** or **2**. (E) Computational simulations of the spatial arrangement of the linkers **1** and **2** within **HSA1** and **HSA2** show that TCOs are accessible for Tz ligations. The structures of **HSA1** and **HSA2** are based on the HSA crystal structure PDB 1N5U.[38] (F) Deconvoluted MS spectra of **Tz-HSA1** and **Tz-HSA2**; (G) radioactive SDS-PAGE gels with $^{111}$In-Tz after exposure to a phosphor plate reveal that $^{111}$In-Tz can react with **HSA1** and **HSA2**. Lane 1–3: **HSA1** with $^{111}$In-Tz, Lane 5–6: **HSA2** with $^{111}$In-Tz, Lane 4 & 7: Native HSA (control) with $^{111}$In-Tz; **HSA1**, **HSA2**, and native HSA were mixed with $^{111}$In-Tz for 1 hour at 37 °C prior to application to the SDS-PAGE gel.

conjugation with **1** or **2** (Fig. 2C). This shows that the $S_NAr$ reaction is orthogonal to the chemistry of the TCO moiety. Moreover, construction of **1** and **2** demonstrates that $S_NAr$ is orthogonal to peptide coupling and CuAAC. To investigate if conjugation with linker **1** and **2** had caused denaturation of HSA, circular dichroism (CD) spectroscopy was carried out of HSA, **HSA1**, and **HSA2** and compared to each other. CD spectroscopy confirmed that conjugation of both linkers did not cause denaturation of HSA, as the α-helical structure of HSA was conserved in **HSA1** and **HSA2** (Fig. 2D).[35]

To model the spatial arrangement of the linkers **1** and **2** within **HSA1** and **HSA2** and to investigate if conjugated TCOs are accessible for Tz ligations, a molecular dynamics simulation was conducted. The HSA crystal structure used for the simulations was PDB 1N5U.[38] The structure of HSA was fixed except for the Cys34 residue (including the protein backbone part) and **1** or **2**, respectively. A solvent sphere with a diameter of 30 Å was placed around the Cys34 residue and **1** or **2**. Repeated cycles of heating/cooling were then conducted to elucidate the preferred conformation of **1** and **2**. The simulations showed that **1** had its olefin double bond at a distance of 17.0 Å from the Cys34 sulfhydryl, whereas for **2**, wrapping of the linker around itself caused the distance between the olefin double bond and the Cys34 sulfhydryl to be 15.0 Å. These simulation results

supported that the linkers indeed had the required lengths and flexibilities for the TCOs to be accessible for Tz ligations (Fig. 2E). Encouraged by these simulations, we aimed to confirm that TCOs are indeed accessible and that TCO moieties still exist in their reactive *trans*-configurations within **HSA1** and **HSA2** after coupling to HSA and purification. We confirmed this by reacting **HSA1** and **HSA2** with 3,6-di(pyrimidin-2-yl)-1,2,4,5-tetrazine to form **HSA3** and **HSA4**, respectively. LC-MS analysis confirmed presence of reactive TCOs and the formation of **HSA3** and **HSA4** (Fig. 2F). Since properties of the linker between the TCO moiety and HSA can influence the kinetics and reactivity of the Tz ligation, both **HSA1** and **HSA2** were examined.[39] Quantification of the reactive TCO load per HSA succeeded *via* SDS-PAGE of **HSA1** and **HSA2** with $^{111}$In-labeled Tz ([$^{111}$In]Tz). On average 0.2 reactive TCO per HSA were available independent on the used shorter, lipophilic linker **1** or the longer, hydrophilic linker **2**. This number is relatively low, but still high enough to selectively introduce any drug or radionuclide into HSA. A 1 : 1 ratio would be preferred but for imaging or radionuclide therapy purposes, a load of 0.2 reactive TCOs per HSA molecule is sufficient as ultra-low concentrations of the radioactive agent are applied.[40–42] For tumor pretargeting, usually 5–7 TCOs per targeting vector are used. With this respect, the TCO load should be further increased for example *via* dendrimers bearing 4–8 TCOs similar to the work published by Zeglis *et al.*[43] The same considerations apply to 'click-to-release' drug release strategies. Native HSA mixed with $^{111}$In-labeled tetrazine was used as control and showed only a radioactive band for the $^{111}$In-Tz. Fig. 2G displays the images of radioactive gel. The gel was exposed on a phosphor screen (MultiSensitive Phosphor Screens) to visualize the radioactive bands on the gel. A band at the molecular weight of ~68 kDa was observed, corresponding to the weight of HSA.

## Conclusion

Herein, we have shown that TCO moieties can easily be introduced using a $S_NAr$ of pentafluorobenzene derivatives. The conjugation did not affect the structural integrity of HSA. LC-MS and SDS-PAGE analysis confirmed that TCOs were active and with an average loading of 0.2 reactive TCOs per HSA molecule. In conclusion, the proposed conjugation strategy is suitable for conventional labeling approaches. For pretargeted strategies as well as for prodrugs strategies the TCO load per HSA has most likely to be increased. Future work is directed into the possibility to introduce more TCOs *via* the proposed method, for example by applying TCO-bearing dendrimers.

## Abbreviations

| | |
|---|---|
| CD | Circular dichroism |
| HSA | Human serum albumin |
| IEDDA | Inverse-electron demand Diels–Alder reaction |
| LC-MS | Liquid chromatography-mass spectrometry |
| MRE | Molar residual ellipticity |
| SDS-PAGE | Sodium dodecyl sulfate-polyacrylamide gel electrophoresis |
| $S_NAr$ | Nucleophilic aromatic substitution |
| TCO | *Trans*-cyclooctene |
| Tz | Tetrazine |

## Conflicts of interest

There are no conflicts to declare.

## Acknowledgements

The authors are grateful for financial support to this project from the Novo Nordisk Foundation (NNF18OC0034734) and the European Union's Horizon 2020 research and innovation programme under the Marie Skłodowska-Curie grant agreement no. 813528.

## References

1 G. Niu, *et al.*, *In vivo* labeling of serum albumin for PET, *J. Nucl. Med.*, 2014, **55**, 1150–1156.
2 B.-A. Jönsson, The History of Nuclear Medicine, in *Handbook of Nuclear Medicine and Molecular Imaging for Physicist*, CRC Press, 2022, vol. 1–15.
3 I. Bedrosian, *et al.*, 99mTc-human serum albumin: an effective radiotracer for identifying sentinel lymph nodes in melanoma, *J. Nucl. Med.*, 1999, **40**, 1143–1148.
4 K. Polom, D. Murawa, P. Nowaczyk, Y. S. Rho and P. Murawa, Breast cancer sentinel lymph node mapping using near infrared guided indocyanine green and indocyanine green–human serum albumin in comparison with gamma emitting radioactive colloid tracer, *Eur. J. Surg. Oncol.*, 2012, **38**, 137–142.
5 L. J. Picker and E. C. Butcher, Physiological and molecular mechanisms of lymphocyte homing, *Annu. Rev. Immunol.*, 1992, **10**, 561–591.
6 S. Karaman and M. Detmar, Mechanisms of lymphatic metastasis, *J. Clin. Invest.*, 2014, **124**, 922–928.
7 E. N. Hoogenboezem and C. L. Duvall, Harnessing albumin as a carrier for cancer therapies, *Adv. Drug Deliv. Rev.*, 2018, **130**, 73–89.
8 H. Lee, *et al.*, 64 Cu-MM-302 Positron Emission Tomography Quantifies Variability of Enhanced Permeability and Retention of Nanoparticles in Relation to Treatment Response in Patients with Metastatic Breast Cancer, *Clin. Cancer Res.*, 2017, **23**, 4190–4202.
9 S. Willhelm, *et al.*, Analysis of nanoparticle delivery to tumours, *Nat. Rev. Mater.*, 2016, **1**, 16014.
10 K. J. Harrington, *et al.*, Effective Targeting of Solid Tumors in Patients With Locally Advanced Cancers by Radiolabeled Pegylated Liposomes, *Clin. Cancer Res.*, 2001, **7**, 243–254.
11 E. J. L. Stéen, *et al.*, Pretargeting in nuclear imaging and radionuclide therapy: Improving efficacy of theranostics and nanomedicines, *Biomaterials*, 2018, **179**, 209–245.

12 Y. Wang, *et al.*, vivo albumin labeling and lymphatic imaging, *Proc. Natl. Acad. Sci. U. S. A.*, 2015, **112**, 208–213.
13 P. F. Spahr and J. T. Edsall, Amino Acid Composition of Human and Bovine Serum Mercaptalbumins, *J. Biol. Chem.*, 1964, **239**, 850–854.
14 V. Lindner and H. Heinle, Binding properties of circulating evans blue in rabbits as determined by disc electrophoresis, *Atherosclerosis*, 1982, **43**, 417–422.
15 M. L. Blackman, M. Royzen and J. M. Fox, Tetrazine ligation: Fast bioconjugation based on inverse-electron-demand Diels-Alder reactivity, *J. Am. Chem. Soc.*, 2008, **130**, 13518–13519.
16 N. K. Devaraj, R. Weissleder and S. A. Hilderbrand, Tetrazine-based cycloadditions: Application to pretargeted live cell imaging, *Bioconjugate Chem.*, 2008, **19**, 2297–2299.
17 R. García-Vázquez, *et al.*, Direct Aromatic 18F-Labeling of Highly Reactive Tetrazines for Pretargeted Bioorthogonal PET Imaging, *Chem. Sci.*, 2021, **12**, 11668–11675.
18 V. Shalgunov, *et al.*, Radiolabeling of a polypeptide polymer for intratumoral delivery of alpha-particle emitter, 225Ac, and beta-particle emitter, 177Lu, *Nucl. Med. Biol.*, 2022, **104–105**, 11–21.
19 M. M. Herth, *et al.*, Development of a 11C-labeled tetrazine for rapid tetrazine-*trans*-cyclooctene ligation, *Chem. Commun.*, 2013, **49**, 3805–3807.
20 E. J. L. Stéen, *et al.*, Improved radiosynthesis and preliminary *in vivo* evaluation of the 11C-labeled tetrazine [11C]AE-1 for pretargeted PET imaging, *Bioorg. Med. Chem. Lett.*, 2019, **29**, 986–990.
21 C. Denk, *et al.*, Development of a 18F-labeled tetrazine with favorable pharmacokinetics for bioorthogonal PET imaging, *Angew. Chem., Int. Ed.*, 2014, **53**, 9655–9659.
22 P. E. Edem, et al., Evaluation of the inverse electron demand Diels-Alder reaction in rats using a scandium-44-labelled tetrazine for pretargeted PET imaging, *EJNMMI Res.*, 2019, **9**, 49.
23 A. Vito, *et al.*, A 99mTc-Labelled Tetrazine for Bioorthogonal Chemistry. Synthesis and Biodistribution Studies with Small Molecule *trans*-Cyclooctene Derivatives, *PLoS One*, 2016, **11**, e0167425.
24 A. Yazdani, *et al.*, Preparation of tetrazine-containing [2 + 1] complexes of 99m Tc and *in vivo* targeting using bioorthogonal inverse electron demand Diels–Alder chemistry, *Dalton Trans.*, 2017, **46**, 14691–14699.
25 M. H. Choi, *et al.*, Highly efficient method for 125I-radiolabeling of biomolecules using inverse-electron-demand Diels–Alder reaction, *Bioorg. Med. Chem.*, 2016, **24**, 2589–2594.
26 T. Läppchen, *et al.*, DOTA-tetrazine probes with modified linkers for tumor pretargeting, *Nucl. Med. Biol.*, 2017, **55**, 19–26.
27 S. Syvänen, *et al.*, Fluorine-18-Labeled Antibody Ligands for PET Imaging of Amyloid-β in Brain, *ACS Chem. Neurosci.*, 2020, **7**, 1–16.
28 R. Rossin, *et al.*, Chemically triggered drug release from an antibody-drug conjugate leads to potent antitumour activity in mice, *Nat. Commun.*, 2018, **9**, 1484.
29 ClinicalTrials.gov, Phase 1 Study of SQ3370 in Patients With Advanced Solid Tumors, 2019, available at: **https://clinicaltrials.gov/ct2/show/NCT04106492**, accessed: 20 April 2022.
30 M. Peplow, Click chemistry sees first use in humans, 2020, available at: **https://cen.acs.org/pharmaceuticals/Click-chemistry-sees-first-use/98/web/2020/10**, accessed: 20 April 2022.
31 S. Srinivasan, *et al.*, SQ3370 Activates Cytotoxic Drug *via* Click Chemistry at Tumor and Elicits Sustained Responses in Injected and Non-Injected Lesions, *Adv. Ther.*, 2021, **4**, 2000243.
32 J. M. J. M. Ravasco, H. Faustino, A. Trindade and P. M. P. Gois, Bioconjugation with Maleimides: A Useful Tool for Chemical Biology, *Chem.–Eur. J.*, 2019, **25**, 43–59.
33 A. M. Embaby, S. Schoffelen, C. Kofoed, M. Meldal and F. Diness, Rational Tuning of Fluorobenzene Probes for Cysteine-Selective Protein Modification, *Angew. Chem. Int. Ed.*, 2018, **130**, 8154–8158.
34 D. Psimadas, V. Valotassiou, S. Alexiou, I. Tsougos and P. Georgoulias, Radiolabeled mAbs as Molecular Imaging and/or Therapy Agents Targeting PSMA, *Cancer Invest.*, 2018, **36**, 118–128.
35 C. W. Tornøe and M. Meldal, Peptidotriazoles: Copper(I)-Catalyzed 1,3-Dipolar Cycloadditions on Solid-Phase, in *Peptides: The Wave of the Future*, ed. M. Lebl and R. A. Houghten, Springer, Dordrecht, 1st edn, 2001, vol. 7, pp. 263–264.
36 C. W. Tornøe, C. Christensen and M. P. Meldal, Peptidotriazoles on solid phase: [1,2,3]-triazoles by regiospecific copper(i)-catalyzed 1,3-dipolar cycloadditions of terminal alkynes to azides, *J. Org. Chem*, 2002, **67**, 3057–3064.
37 V. V. Rostovtsev, L. G. Green, V. V. Fokin and K. B. Sharpless, A Stepwise Huisgen Cycloaddition Process: Copper(i)-Catalyzed Regioselective "Ligation" of Azides and Terminal Alkynes, *Angew. Chem. Int. Ed.*, 2002, **41**, 2596–2599.
38 M. Wardell, *et al.*, The Atomic Structure of Human Methemalbumin at 1.9 Å, *Biochem. Biophys. Res. Commun.*, 2002, **291**, 813–819.
39 R. Rossin, S. M. J. Van Duijnhoven, T. Läppchen, S. M. Van Den Bosch and M. S. Robillard, Trans-cyclooctene tag with improved properties for tumor pretargeting with the Diels-Alder reaction, *Mol. Pharm.*, 2014, **11**, 3090–3096.
40 K. T. Chen, *et al.*, Ultra–Low-Dose 18 F-Florbetaben Amyloid PET Imaging Using Deep Learning with Multi-Contrast MRI Inputs, *Radiology*, 2019, **290**, 649–656.
41 K. Khamwan, A. Krisanachinda and P. Pasawang, The determination of patient dose from 18F-FDG PET/CT examination, *Radiat. Prot. Dosim.*, 2010, **141**, 50–55.
42 R. W. Rawson, J. E. Rall and W. Peacock, Limitations and Indications In The Treatment of Cancer Of The Thyroid With Radioactive Iodine, *J. Clin. Endocrinol. Metab.*, 1951, **11**, 1128–1142.
43 B. E. Cook, R. Membreno and B. M. Zeglis, Dendrimer Scaffold for the Amplification of *in Vivo* Pretargeting Ligations, *Bioconjugate Chem.*, 2018, **29**, 2734–2740.